Direct Fit for SVI Implied Volatilities

Wolfgang Schadner*

August 23, 2023

Abstract

The stochastic volatility inspired (SVI) formula is one of the mainstream models for fitting the option implied volatility smile. Herein I fully linearize the SVI equation by rewriting it into the algebraic form of a conic section, limited to the geometric shape of a hyperbola. This step reduces the complexity of the otherwise non-linear optimization problem significantly. Based on the conic representation, I introduce the direct least-squares for SVI, allowing us to fit the model in a computationally efficient and non-iterative manner. The performance of the proposed method is evaluated upon empirical data of seven different asset classes. It turns out to deliver a very good fit, and is about 25 times faster than the existing 'quasi-explicit' benchmark algorithm. Following the outstanding computational speed combined with the high accuracy, the direct SVI fit qualifies as a robust method for calibrating implied volatilities in real-time, and for applications to big option datasets.

Keywords: implied volatility, volatility smile, calibration, SVI, hyperbola, high-frequency
JEL: C58, G12, C61

1 Introduction

The *stochastic volatility inspired* (SVI) formula was introduced by Jim Gatheral in 2004 [5]. It quickly became one of the leading references for implied volatility modeling due to its inherent simplicity, asymptotic relation to stochastic volatility models (like Heston, cf. [4, 7]), and its virtually arbitrage-free nature (cf. [3]). Not only does it enjoy an ongoing vivid academic discussion [8, 10, 16, 17], it also became widely recognized within the practitioners literature [2, 13, 14] and found its way as a prime example into finance textbooks [6, 9]. Given option contracts of same maturity, Gatheral's [5] original 'raw' parameterization is defined as

$$\omega = a + b\left[\rho(x-m) + \sqrt{(x-m)^2+\sigma^2}\right] \tag{1}$$

*Liechtenstein Business School. This project was mainly conducted during the author's former affiliation with the University of St. Gallen and visiting stay at the Harvard Business School. E-Mail: wolfgang.schadner@uni.li. Web: www.w-schadner.com

with ω as the total implied variance for the level of forward log-moneyness x, and $\{a, b, \rho, m, \sigma\} \in \mathbb{R}$ as the five model parameters. The total implied variance per se follows the standard notation of $\omega = \tau\sigma_{BS}(x)^2$, having $\sigma_{BS}(x)$ as the Black-Scholes implied volatility. Obviously, the SVI formula in its raw notation (Eq.1) describes a non-linear relationship, hence is traditionally calibrated via iterative optimization routines. These algorithms are typically computationally expensive, and get easily stuck in sub-optimal local minima due to their sensitivity to the initial parameter choice. It is therefore generally preferred to linearize optimization problems whenever feasible. And this is precisely what I discuss within this work.

A partial linearization was already introduced by [15], which became a calibration reference on its own as it significantly reduced the problem from a five-, down to a two-parameter optimization problem. Different to this quasi-explicit solution I derive a simple, non-iterative method. The key to my approach lies in recognizing the SVI formula as a conic section, with only hyperbolic or flat geometric shapes being feasible. Leveraging the conic representation, I draw upon fitting methods from the pattern recognition literature, and calibrate Eq.1 by minimizing the algebraic distance between the conic and the data. The very same concept can be used for the vanishing SVI (flat extrapolation) and the SSVI model. I evaluate the performance of the direct least-squares method upon empirical option data for seven different asset classes: equity (S&P 500 index), fixed income (10 year Treasury Note), foreign exchange (EUR/USD rate), cryptocurrency (Bitcoin), metals (gold), oil (WTI) and agriculture (wheat). These calibration experiments demonstrate a qualitatively high fit of the proposed method alongside an outstanding fast computational speed. In direct comparison with the quasi-explicit routine, the direct least-squares is about 25 times faster (mean latency of 0.087 vs. 2.131 milliseconds in the setting herein) at a comparable level of sum-of-squared-errors. Therefore, the proposed method appears promising for the analysis of large option data sets, as well as calibrating implied volatilities and risk-neutral densities in real-time.

2 Summary of the Algorithm

1. Start with the design matrix $D = \begin{pmatrix} \mathbf{x}^2 & \boldsymbol{\omega}^2 & \mathbf{x}\boldsymbol{\omega} & \mathbf{x} & \boldsymbol{\omega} & \mathbf{1} \end{pmatrix}$.
2. Compute the (weighted) scatter matrix $S = D'WD$. Partition it into the sub-matrices S_{cc}, S_{uc} and S_{uu} to calculate $M = S_{cc} - S'_{uc}S_{uu}^{-1}S_{uc}$.
3. Estimate the conic coefficients $\mathbf{z} = \begin{pmatrix} \mathbf{z}_c & \mathbf{z}_u \end{pmatrix}'$ from Eqs.21 and 17.
4. (optional) Apply the low eccentricity correction of [11].
5. Get estimated ω from Eq.7, or translate $\mathbf{z}$ back into the original SVI parameters via Eq.5.

3 Geometric Background

The SVI equation is loosely referred to as a hyperbola (e.g., [19]), and this section elaborates on the geometric aspect in greater detail. We will see that understanding the geometric nature of SVI is advantageous as it allows us to borrow sophisticated fitting algorithms that were developed within other scientific disciplines. Geometrically speaking, the hyperbola is a sub-class of the quadratic forms in the projective plane, also known as conic sections. The algebraic definition of such is written as

$$\mathbf{dz} = \begin{pmatrix} x^2 & \omega^2 & x\omega & x & \omega & 1 \end{pmatrix} \begin{pmatrix} z_1 & z_2 & z_3 & z_4 & z_5 & z_6 \end{pmatrix}' = 0 \tag{2}$$

(see [18]) with the 'design' vector $\mathbf{d}$ and the conic coefficients $\mathbf{z}$. The quadratic terms of $\mathbf{z}$ thereby play an important role as they distinguish the three possible conics:

$$z_3^2 - 4z_1z_2 \begin{cases} > 0 \ldots \text{ hyperbola} \\ = 0 \ldots \text{ parabola (or linear)} \\ < 0 \ldots \text{ ellipse} \end{cases} \tag{3}$$

Theorem 3.1. *The SVI formula (Eq.1) resembles a conic section.*

Proof. The square-root within Eq.1 fades away when rearranging terms and taking squares,

$$[\omega - a - b\rho(x-m)]^2 = b^2[(x-m)^2 + \sigma^2] \tag{4}$$

. Next, expanding the above equation, bringing all terms to the LHS, and defining the conic coefficients as

$$\mathbf{z} := \begin{pmatrix} b^2(\rho^2-1) \\ 1 \\ -2b\rho \\ 2mb^2 - 2b\rho(b\rho m - a) \\ 2(b\rho m - a) \\ (b\rho m - a)^2 - b^2(m^2+\sigma^2) \end{pmatrix} \tag{5}$$

results in

$$z_1x^2 + z_2\omega^2 + z_3x\omega + z_4x + z_5\omega + z_61 = 0 \tag{6}$$

which is identical to Eq.2. □

The great advantage of the conic representation is that it fully linearizes the otherwise non-linear SVI formula, which, in turn, makes it attractive for fitting purposes. Alternatively to Eq.1, the SVI formula can

be expressed in terms of the conic coefficients,

$$\omega = \frac{1}{2z_2}\left[-(z_3x + z_5) + \sqrt{(z_3x + z_5)^2 - 4z_2(z_1x^2 + z_4x + z_6)}\right] \tag{7}$$

.[1] Next, by Theorem 3.2 we are able to identify the possible shapes of SVI, which is necessary to understand the feasible range of the coefficients $\mathbf{z}$.

Theorem 3.2. *Given the SVI parameters $\{a, b, \rho, m, \sigma\}$ are real, the SVI model produces only two different shapes: flat or hyperbolic.*

Proof. Follows from Lemma 3.1-3.3. □

Lemma 3.1. *The SVI model produces a hyperbolic shape if, and only if, $b \neq 0$.*

Proof. Take Eq.3 and substitute for Eq.5. What we observe is

$$b^2 = \tfrac{1}{4}z_3^2 - z_1z_2 \tag{8}$$

Hence, with $b \in \mathbb{R}$ and $b \neq 0$ it follows that $0 < b^2 \implies z_3^2 - 4z_1z_2 > 0$. Therefore, from Eq.3 we know that SVI resembles a hyperbola whenever $b \neq 0$. □

Lemma 3.2. *The SVI model has no parabolic solution.*

Proof. From Eqs.3 and 8 we know that $b = 0$ is necessary for SVI to produce a parabolic shape. However, by Eq.1 we recognize that $b = 0$ implies $\forall x : \omega(x) = a$. Hence, $b = 0$ produces the flat Black-Scholes implied volatility surface, but certainly not a parabola. □

Lemma 3.3. *The SVI model has no elliptic solution.*

Proof. Since $b \in \mathbb{R}$ it follows that $b^2 \geq 0$. Therefore, given Eq.8, we know that $z_3^2 - 4z_1z_2 < 0$ does not exist within the SVI framework. □

The conic equation of Eq.6 can be arbitrarily scaled. In Proposition 3.1 we observe that this is particularly useful for introducing new parameter constraints.

Proposition 3.1. *A necessary condition for the positivity of ω is that $\rho \in [-1, 1]$ (cf. [16]), which holds whenever $-z_1z_2 \geq 0$.*

Proof. This can be seen when normalizing $\mathbf{z}$ by z_3. Let the normalized coefficients be denoted by $\tilde{\mathbf{z}}$, from which follows that $-4\tilde{z}_1\tilde{z}_2 = \frac{1-\rho^2}{\rho^2}$. Therefore, $-z_1z_2 \geq 0$ implies $\rho \in [-1, 1]$ and vice versa. □

[1] Eq.7 is a quadratic equation with two solutions for ω (i.e., $\pm\sqrt{\ldots}$). However, by the convexity of implied variance, only the upper solution is relevant.

The constraint of $\rho \in [-1, 1]$ describes that $\lim_{x\to\infty} \omega(x)$ converges towards a non-negatively sloped branch, and $\lim_{x\to-\infty} \omega(x)$ to a negatively sloped (or flat) branch. Hence, is obligatory for ω being convex and positive. With an eye on Eq.3 we recognize that $-z_1 z_2 \geq 0$ strictly produces a subset of possible hyperbolas. For fitting the SVI equation it is thus useful to limit ρ to ± 1, and work with the more stringent constraint of $-z_1 z_2 \geq 0$ instead of Eq.3. Proposition 3.1 should be also considered when using other conic fitting algorithms than the proposed direct least-squares below.

3.1 Vanishing SVI

The vanishing SVI is a sub-model of Eq.1, and is defined as the implied variance surface becoming flat within the left or the right wing (cf. [16]). As for the parameterization this means that $\rho = \pm 1$, and is achieved by setting $z_1 = 0$. With respect to Eq.3 we recognize that this strictly produces a hyperbolic shape (or flat if $z_3 = 0$). Therefore, the vanishing SVI can be directly fit by an unconstrained ordinary least-squares with $-\omega^2$ as the dependent variable, and the remaining terms (excluding x^2) as the explanatory variables. The sign of ρ is thereby automatically detected and the fitted variance will converge towards the parameter a at $x \to \pm\infty$. Note that a represents the minimum of ω only in the vanishing SVI model, but not for the general cases where $|\rho| < 1$. For the vanishing SVI it is also possible to pre-specify the parameter a while still fitting the model with an unconstrained OLS. In that case, the dependent variable is $\{-(\omega - a)^2\}$ and the three explanatory variables are $\{(\omega - a)x,\ \omega,\ 1\}$. When using $\mathbf{z}_v$ to denote the regression coefficients, then the link to the original SVI parameters is given by

$$\begin{pmatrix} b & \rho & m & \sigma \end{pmatrix} = \begin{pmatrix} \frac{1}{2}|z_{v,1}| & \frac{z_{v,1}}{|z_{v,1}|} & \frac{z_{v,3}}{z_{v,1}} & 2\sqrt{-\frac{a z_{v,3} + z_{v,2}}{|z_{v,1}|}} \end{pmatrix} \tag{9}$$

3.2 SSVI

The surface SVI (or SSVI) is another sub-model introduced by [8]. Its key advantage is that it has traceable conditions under which it produces an arbitrage-free volatility surface. The model is defined by

$$\omega = \frac{\theta}{2}\left(1 + \rho\phi x + \sqrt{(\phi x + \rho)^2 + 1 - \rho^2}\right) \tag{10}$$

. Also this model can be easily linearized via the algebraic conic representation, with the SSVI-parameters being linked to $\mathbf{z}$ via

$$\begin{pmatrix} z_1 \\ z_2 \\ z_3 \end{pmatrix} = \begin{pmatrix} \frac{1}{4}\theta^2\phi^2(\rho^2 - 1) \\ 1 \\ -\theta\rho\phi \end{pmatrix} \quad \text{and} \quad \begin{pmatrix} z_4 \\ z_5 \\ z_6 \end{pmatrix} = \begin{pmatrix} 0 \\ -\theta \\ 0 \end{pmatrix} \tag{11}$$

. Therefore, the SSVI model be calibrated to implied variance slices directly just like the general SVI.

4 Direct Least-Squares

While several different algorithms exist for fitting conics/hyperbolas, the one I present herein is based on [18]'s direct type-specific least-squares, minimizing the algebraic distance (Eq.6). I modify the original method to the extent of matching the SVI-specific requirements. With that in mind, let $\mathbf{x}$ and $\boldsymbol{\omega}$ define our input data (vectors of x's and ω's), captured by the design matrix D as

$$D = \begin{pmatrix} \mathbf{x}^2 & \boldsymbol{\omega}^2 & \mathbf{x}\boldsymbol{\omega} & \mathbf{x} & \boldsymbol{\omega} & \mathbf{1} \end{pmatrix} \tag{12}$$

. Analogously to Eq.2, the error term is given as $\epsilon = D\mathbf{z}$. The conic coefficients are now split into the constrained $\mathbf{z}_c = \begin{pmatrix} z_1 & z_2 \end{pmatrix}'$ and the unconstrained $\mathbf{z}_u = \begin{pmatrix} z_3 & z_4 & z_5 & z_6 \end{pmatrix}'$ parts. The coefficient z_2 will be set to 1 in a later step. Next, I introduce the constrain matrix C to express the quadratic constraint upon $\mathbf{z}_c$ as

$$\mathbf{z}_c' C \mathbf{z}_c \geq 0 \qquad \text{where} \qquad C = \begin{pmatrix} 0 & -\frac{1}{2} \\ -\frac{1}{2} & 0 \end{pmatrix} \tag{13}$$

to ensure that the fitted solution resembles a feasible hyperbola. While I defined C according to Proposition 3.1, it is also possible to introduce alternative parameter constraints by formulating C differently. This is also the reason why I present the more general solution first, before setting $z_2 = 1$.

In real world applications it is common practice to put a higher weight on options that are closer to the at-the-money level than on far out-of-the money options.[2] Such a weighted least-squares can be incorporated by introducing a diagonal matrix W, with the desired weights on the diagonal. Our optimization problem is now formally expressed as:

$$\min \{\mathbf{z}' D' W D \mathbf{z}\} \quad \text{s.t.} \quad \mathbf{z}_c' C \mathbf{z}_c \geq 0 \tag{14}$$

. For the subsequent steps it is convenient to introduce the scatter matrix $S := D'WD$ to keep notation tidy. The scatter matrix itself can be partitioned into sub-matrices with respect to the constrained c and

[2] Because illiquidity and the likelihood of mispricing increases the further the option is out-of-the-money. A common weighting regime among practitioners is to use the option vega.

unconstrained parts u.[3] With that in mind, the Lagrangian function writes as

$$\mathcal{L} = \begin{pmatrix} \mathbf{z}_c & \mathbf{z}_u \end{pmatrix} \underbrace{\begin{pmatrix} S_{cc} & S'_{uc} \\ S_{uc} & S_{uu} \end{pmatrix}}_{=S} \begin{pmatrix} \mathbf{z}_c \\ \mathbf{z}_u \end{pmatrix} - \lambda \mathbf{z}'_c C \mathbf{z}_c \tag{15}$$

with the partial derivatives set to zero for the optimal solution(s):

$$\frac{\partial \mathcal{L}}{\partial \mathbf{z}_c} \overset{\text{set}}{=} 0 : \qquad S_{cc}\mathbf{z}_c + S'_{uc}\mathbf{z}_u - \lambda C \mathbf{z}_c = 0 \tag{16}$$

$$\frac{\partial \mathcal{L}}{\partial \mathbf{z}_u} \overset{\text{set}}{=} 0 : \qquad S_{uc}\mathbf{z}_c + S_{uu}\mathbf{z}_u = 0 \quad \Longrightarrow \; \mathbf{z}_u = -S_{uu}^{-1} S_{uc} \mathbf{z}_c \tag{17}$$

. When defining $M := S_{cc} - S'_{uc} S_{uu}^{-1} S_{uc}$, then from $\frac{\partial \mathcal{L}}{\partial \mathbf{z}_c} = 0$ follows that

$$C^{-1} M \mathbf{z}_c = \lambda \mathbf{z}_c \tag{18}$$

which represents a classic eigenvalue problem. When working with the more stringent constraint $-z_1 z_2 > 0$, however, then we can spare us the eigendecomposition for the computation of $\mathbf{z}_c$. Set $z_2 = 1$ and consider that $M\mathbf{z}_c = \lambda C \mathbf{z}_c$ can be split into

$$M_{11} z_1 + M_{12} = \lambda (C_{11} z_1 + C_{12}) \qquad \text{and} \qquad M_{21} z_1 + M_{22} = \lambda (C_{21} z_1 + C_{22}) \tag{19}$$

. Substituting for the values of C and rearranging terms, it follows that z_1 has two optimal solutions, an elliptic and a hyperbolic one:

$$z_{1,\pm} = \pm \sqrt{\frac{M_{22}}{M_{11}}}, \tag{20}$$

. By Theorem 3.2 we know that the negative z_1 is our desired estimate; it represents the global hyperbolic optimum that minimizes the algebraic distance of the SVI formula. Hence, once the optimal

$$\mathbf{z}_c = \begin{pmatrix} -\sqrt{\frac{M_{22}}{M_{11}}} & 1 \end{pmatrix}' \tag{21}$$

is known, the remaining conic coefficients $\mathbf{z}_u$ can be recovered from Eq.17.

At this point it should be mentioned that the above method minimizes the algebraic distance, which became subject to critique (e.g., [12]). It is possible to further improve the geometric fit, for example by applying the - also non-iterative - low eccentricity correction of [11] or noise cancellation of [12].

[3] $S_{cc} = S_{1:2,1:2}$, $S_{uc} = S_{3:6,1:2}$, and $S_{uu} = S_{3:6,3:6}$. When working with the more general constraint of $z_3^2 - 4z_1 z_2 > 0$, then the corresponding constraint matrix writes $C = \left(\begin{smallmatrix} 0 & -2 & 0 \\ -2 & 0 & 0 \\ 0 & 0 & 1 \end{smallmatrix}\right)$ with c/u relating to the elements 1:3/4:6; see [18] for further details.

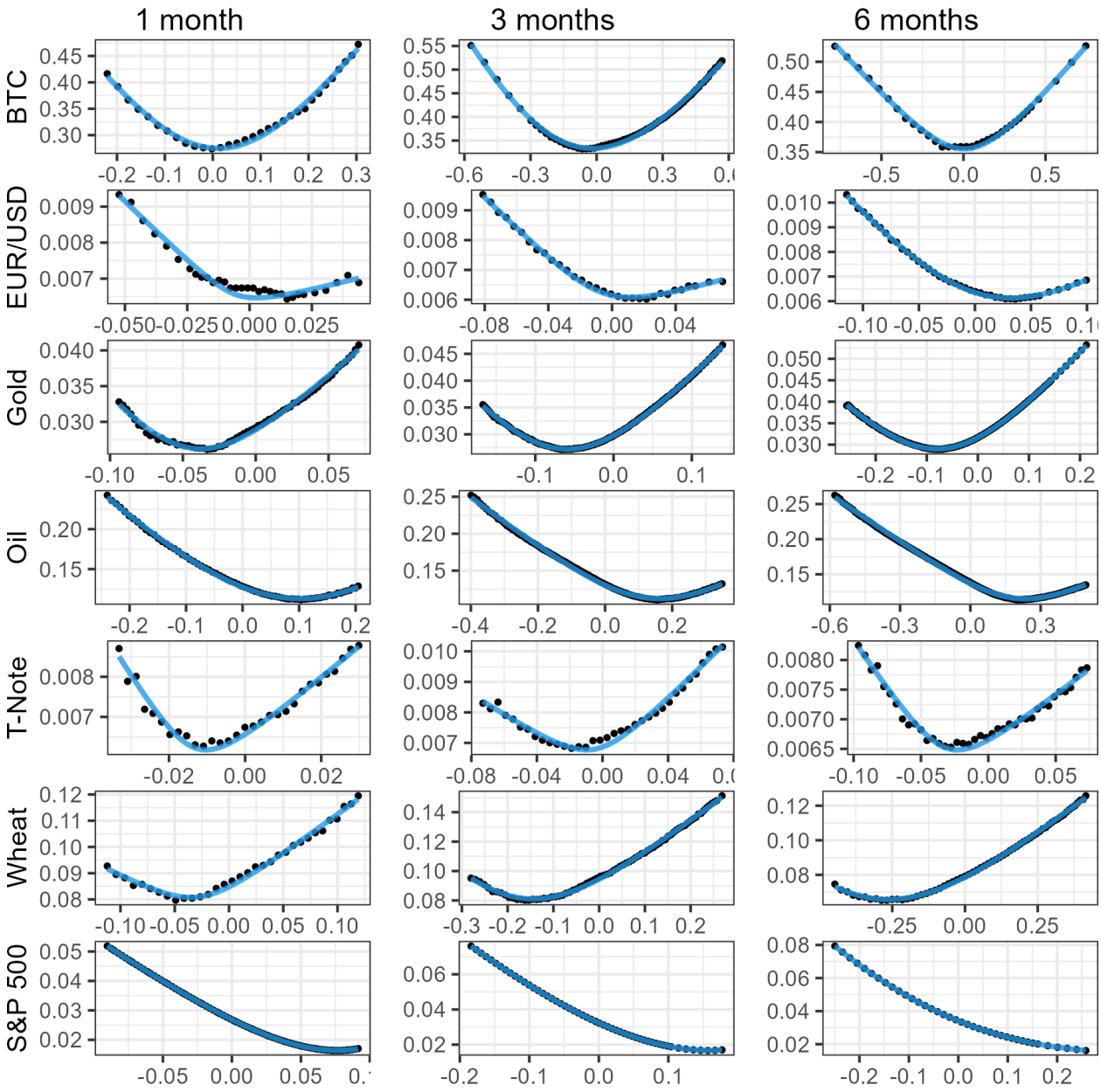

Figure 1: Calibration experiments of the direct SVI fit (blue line) for various asset classes (rows) and maturities (columns); implied variance ω on y-axis, log-moneyness x on x-axis. The presented method delivers a reliable and high goodness-of-fit on all of the 21 examples.

5 Calibration Experiments

The empirical applicability of the direct least-squares is tested upon various different samples. The asset classes represented are equity (S&P 500 index), cryptocurrency (Bitcoin), foreign exchange (EUR/USD rate), metals (gold), commodities (WTI oil), bonds (10-year Treasury Note) and agriculture (wheat). The target maturities of the option contracts are approximately one-, three-, and six months. The end-of-day closing prices are collected from CME's DataMine (accessed via QuickStrike) as of 4/7/2023. The calibrations are made upon out-of-the-money put- and call options only. Given that far OTM options are prone to mispricing (e.g., due to illiquidity) I only consider contracts that lie within the range of two at-the-money standard deviations (i.e., approximately 95% of the risk-neutral density distribution).

Fig.1 displays the 21 implied variance slices together with the estimated fits of the direct least-squares. Visual inspection reveals that it produces a high goodness-of-fit in all of the examples. Hence, the SVI formula can be efficiently calibrated to empirical data without the requirement of iterative algorithms. Tab.1 reports the aggregated results on computational time, the sum of squared errors SSE, and the percentage of arbitrage-free fits as measured upon violation of the Durrleman condition (cf. [16]). The column *direct* refers to the proposed direct fit, *direct+ec.* additionally applies the low eccentricity correction of [11], and *quasi-ex.* relates to the quasi-explicit solution of [15], which is widely considered as the fastest SVI calibration algorithm so far (e.g., [16]). Note that the latter is an iterative algorithm, thus sensitive to the initial parameter choice of μ_0 and σ_0. Therefore, the computational experiment is repeated under different starting values for this routine.[4] All computations were carried out on a conventional notebook with an Intel(R) Core(TM) i5 @ 2.4 GHz, quad-core processor using the statistical programming software `R`. The insights from the calibration experiments are as follows. The computational time for the direct fit ranged between 0.077 and 0.129 milliseconds, at an average of 0.087. To put these numbers into context, consider that sophisticated high-frequency trading firms execute trades on a time-scale of milli- or even microseconds (see e.g., [1]). Hence, already under my 'slow' soft- and hardware setting, the direct SVI fit performed at a speed that is competitive for real-time applications. When adding the low eccentricity correction, then the computation time increases by around 40%. In contrast, the quasi-explicit calibration takes significantly longer and is on average 25 times slower than the direct one. It is also exposed to the risk of getting stuck in substantially longer computation times, where the longest calibration time within the experiments took around 94 milliseconds (vs. 0.129 at *direct*). In terms of goodness-of-fit as measured upon SSE, however, the differences are less drastic. The average SSE of *direct* is around 40% higher than that of *quasi-ex.*, and the gap is largely removed when combining the direct fit with the low eccentricity correction. On the other hand, while *quasi-ex.* tends to better minimize SSE on average, we also see that it is sensitive to the initial parameter choice as the maximum SSE is larger than that of *direct*. Hence, *quasi-ex.* occasionally converges

[4] More precisely, starting values are $\mu_0 = \{-0.5, -0.4, ..., 0.5\}$ and $\sigma_0 = \{0.05, 0.1, ..., 1\}$. The quasi-explicit algorithm is fitted using `R`'s `optim` function with the L-BFGS-B (quasi-Newton) optimization routine.

towards an unpleasant local minimum. At the aspect of arbitrage-freeness it is also *quasi-ex.* to perform worst. A potential explanation for that is an over-fitting of mispriced options.

Table 1: Results from calibrating the SVI formula to the 21 samples of different asset classes. Compared methods are (i) the presented direct fit, (ii) direct fit plus low eccentricity correction of [11], and (iii) the quasi-explicit solution of [15]. The direct fitting methods perform significantly faster while achieving a similar goodness-of-fit.

	absolute			normalized		
	direct	direct+ec.	quasi-ex.	direct	direct+ec.	quasi-ex.
	computation time [ms]					
min	0.077	0.108	0.274	1	1.403	3.558
mean	0.087	0.123	2.131	1	1.414	24.48
max	0.129	0.189	93.73	1	1.465	726.6
	error: SSE $\times 10^5$					
min	0.001	0.001	0.001	1.014	1	1.000
mean	8.955	6.862	6.392	1.305	1	0.932
max	65.14	36.59	84.46	1.780	1	2.309
	arbitrage-free					
$\min\{\text{Durr.}\} > 0$	76.2%	52.4%	25.6%			

6 Conclusion

In this work I formally identify the SVI equation as a conic section. The insight allows to fully linearize the otherwise non-linear equation, and to borrow sophisticated fitting algorithms that were developed within other scientific disciplines (like image processing, pattern recognition). By minimizing the algebraic distance I demonstrate that the SVI equation can be fit in a direct, non-iterative manner. This closed-form solution is simple and, when compared to existing SVI fitting algorithms, comes with two key advantages: First, it is highly computationally efficient, allowing to fit the SVI equation in real-time. Second, it is insensitive to the initial parameter choice as it identifies the global optimum. From calibration experiments across seven different asset classes I observe a satisfying good fit to empirical data. And in terms of computational speed, the direct fit significantly outperforms the quasi-explicit solution of [15], which is widely considered as the fastest SVI fitting algorithm so far. From the observed results I believe the proposed method to have a great potential for applications in high-frequency trading and processing large option data sets; and the usage of conic fitting algorithms in general to be a promising new approach for efficient calibrations of implied volatility surfaces.

References

[1] Baron, M., Brogaard, J., Hagströmer, B. and Kirilenko, A. [2019], 'Risk and return in high-frequency trading', *Journal of Financial and Quantitative Analysis* **54**, 993–1024.

[2] Damghani, B. M. and Kos, A. [2013], 'De-arbitraging with a weak smile: Application to skew risk', *Wilmott* **1**, 40–49.

[3] Floc'h, F. L. and Oosterlee, C. W. [2019], 'Model-free stochastic collocation for an arbitrage-free implied volatility: Part i', *Decisions in Economics and Finance* **42**, 679–714.

[4] Friz, P., Gerhold, S., Gulisashvili, A. and Sturm, S. [2011], 'On refined volatility smile expansion in the heston model', *Quantitative Finance* **11**, 1151–1164.

[5] Gatheral, J. [2004], 'A parsimonious arbitrage-free implied volatility parameterization with application to the valuation of volatility derivatives', *Presentation at Global Derivatives & Risk Management* .

[6] Gatheral, J. [2011], *The volatility surface: a practitioner's guide*, John Wiley & Sons.

[7] Gatheral, J. and Jacquier, A. [2011], 'Convergence of heston to svi', *Quantitative Finance* **11**, 1129–1132.

[8] Gatheral, J. and Jacquier, A. [2014], 'Arbitrage-free svi volatility surfaces', *Quantitative Finance* **14**, 59–71.

[9] Gulisashvili, A. [2012], *Analytically Tractable Stochastic Stock Price Models*, Springer.

[10] Guo, G., Jacquier, A., Martini, C. and Neufcourt, L. [2016], 'Generalized arbitrage-free svi volatility surfaces', *SIAM Journal on Financial Mathematics* **7**, 619–641.

[11] Harker, M., O'leary, P. and Zsombor-Murray, P. [2008], 'Direct type-specific conic fitting and eigenvalue bias correction', *Image and Vision Computing* **26**, 372–381.

[12] Hunyadi, L. and Vajk, I. [2014], 'Constrained quadratic errors-in-variables fitting', *The Visual Computer* **30**, 1347–1358.

[13] Itkin, A. [2014], 'One more no-arbitrage parametric fit of the volatility smile', *arXiv* .
URL: *arxiv.org/abs/1407.0256v1*

[14] Itkin, A. [2020], *Fitting Local Volatility: Analytic and Numerical Approaches in Black-Scholes and Local Variance Gamma Models*, World Scientific.

[15] Marco, S. D. and Martini, C. [2009], 'Quasi-explicit calibration of gatheral's svi model', *Zeliade White Paper* pp. 1–15.

[16] Martini, C. and Mingone, A. [2022], 'No arbitrage svi', *SIAM Journal on Financial Mathematics* **13**, 227–261.

[17] Nagy, L. and Ormos, M. [2019], 'Volatility surface calibration to illiquid options', *The Journal of Derivatives* **26**, 87–96.

[18] O'Leary, P. and Zsombor-Murray, P. [2004], 'Direct and specific least-square fitting of hyperbolæ and ellipses', *Journal of Electronic Imaging* **13**, 492–503.

[19] Wystup, U. [2020], 'The minimum of the smile fit is not even in the market!', *Wilmott Magazine* .